

# Molecular-dynamics simulation of model polymer nanocomposite rheology and comparison with experiment

T. Kairn and P. J. Daivis<sup>a)</sup>

Department of Applied Physics, School of Applied Sciences, Royal Melbourne Institute of Technology (RMIT) University, G.P.O. Box 2476V, Melbourne, Victoria 3001, Australia

I. Ivanov and S. N. Bhattacharya

Rheology and Materials Processing Centre, Royal Melbourne Institute of Technology (RMIT) University, G.P.O. Box 2476V, Melbourne, Victoria 3001, Australia

(Received 25 July 2005; accepted 12 September 2005; published online 14 November 2005)

The shear-rate dependence of viscosity is studied for model polymer melts containing various concentrations of spherical filler particles by molecular-dynamics simulations, and the results are compared with the experimental results for calcium-carbonate-filled polypropylene. Although there are some significant differences in scale between the simulated model polymer composite and the system used in the experiments, some important qualitative similarities in shear behavior are observed. The trends in the steady-state shear viscosities of the simulated polymer-filler system agree with those seen in the experimental results; shear viscosities, zero-shear viscosities, and the rate of shear thinning are all seen to increase with filler content in both the experimental and simulated systems. We observe a significant difference between the filler volume fraction dependence of the zero-shear viscosity of the simulated system and that of the experimental system that can be attributed to a large difference in the ratio of the filler particle radius to the radius of gyration of the polymer molecules. In the simulated system, the filler particles are so small that they only have a weak effect on the viscosity of the composite at low filler volume fraction, but in the experimental system, the viscosity of the composite increases rapidly with increasing filler volume fraction. Our results indicate that there exists a value of the ratio of the filler particle radius to the polymer radius of gyration such that the zero-shear-rate viscosity of the composite becomes approximately independent of the filler particle volume fraction.

© 2005 American Institute of Physics. [DOI: [10.1063/1.2110047](https://doi.org/10.1063/1.2110047)]

## I. INTRODUCTION

Nanostructured polymer composites currently hold great interest for materials science. Displaying improved strength, fire-retardancy, and barrier properties over simple polymers, polymer nanocomposites have the potential to find many applications. The control of the engineering and fabrication processes involved in the production and use of these materials requires a detailed understanding of their rheological behavior.

Various polymer composites have been examined previously through experiment<sup>1–3</sup> and simulations.<sup>4–8</sup> However, we aim to link simulation with experiment, comparing an original set of molecular-dynamics (MD) simulation data to some new experimental results, thereby demonstrating the usefulness of the MD method in predicting broad qualitative trends in nanocomposite rheology.

Our simulation-based study examines comparatively short model polymer chains of 20 interaction sites. To a series of these short-chain polymer melts are added with various concentrations of spherical nanofiller particles which have a diameter of  $d=2.2254\sigma$ , where  $\sigma$  is the interparticle separation at which the Lennard-Jones interaction energy is a

minimum (see Sec. II A 1). This simulated system approximately represents a polypropylene with a molar mass  $M \approx 2200$  g/mol and a filler with a particle diameter  $d \approx 1.55$  nm.

The application of a similarly coarse-grained polymer model to the simulation of a polymer composite can be found in previous work,<sup>4,7</sup> where a bead-spring model polymer melt is simulated in the process of intercalating between model platelets. A coarse-grained bead-spring polymer chain is also used in the molecular-dynamics study of Smith *et al.*<sup>5</sup> on spherical nanoparticle interactions in a polymer composite. Smith *et al.* observed that the strength of the interaction between polymer and filler can affect the dispersion of filler through the polymer matrix and that increasing the molecular weight of the polymer leads to filler aggregation. However, the possible rheological effects of these structural changes were not examined in their study nor was the influence of filler concentration.

Simulation studies of the rheological properties of polymer composites are rare. There have been some recent interest in simulating the structure and dynamics of composites containing carbon nanotubes (see Frankland *et al.*,<sup>6</sup> for example), and Starr *et al.*<sup>8</sup> have investigated the effect of filler particle clustering on the rheology of a polymer melt. They found that the viscosity of the composite increases with

<sup>a)</sup>Author to whom correspondence should be addressed. Electronic mail: [peter.daivis@rmit.edu.au](mailto:peter.daivis@rmit.edu.au)

increasing dispersion of the filler particles, in general agreement with experimental results, but in disagreement with expectations based on the behavior of typical colloidal dispersions. In the current study, we use molecular-dynamics simulations to describe the shear-rate dependence of the viscosity for polymer composites containing a range of concentrations of spherical filler particles. An important difference between the simulations of Starr *et al.*<sup>8</sup> and our simulations is that in their simulations, an adjustable attraction between polymer and nanoparticle interaction sites is included, whereas we study a model in which both polymer and nanoparticle interactions are purely repulsive.

The results of our simulations are compared with an experimental analysis of a real polymer filled with spherical nanoparticles. The experimental system contains much longer polymers, as well as filler particles which are as much as 45 times larger than those simulated. Despite these considerable differences of scale, this study aims to illustrate a general qualitative agreement between the forms of the shear viscosity versus strain rate curves observed via experiment and simulation.

Kao and Bhattacharya<sup>9</sup> observed that polymer melts filled with spherical particles have greater viscosity than the unfilled polymer at all shear rates examined, and that the viscosity increases with filler concentration. These observations are reflected in the results of various studies of polymers filled with nonspherical particles.<sup>1-3,10</sup> Clay microplatelets have been shown to increase the viscosity of polymer melts when added at low concentrations<sup>2,3,10</sup> and to very significantly alter the rheology of the polymer when more concentrated.<sup>1,2</sup> It has been proposed<sup>2,3</sup> that the increase in polymer-clay composite viscosity with clay content is related to the increase in interactions between polymer chains and clay platelets. Choi *et al.*<sup>2</sup> made this argument in terms of the resistance to the polymer flow generated by the intervention of clay in the polymer matrix.

The current study aims to address these issues while showing how molecular-dynamics simulations can produce steady-state shear behavior very similar to that observed in an experimental system.

## II. METHODS

### A. Simulation method

#### 1. Molecular model

The 20-site polymer molecule model simulated in this study has been examined previously.<sup>11,12</sup> The molecules are modeled by chains of 20 spherical interaction sites, where each site interacts via the Weeks-Chandler-Andersen (WCA) potential, which is a truncated, shifted form of the Lennard-Jones (LJ) potential (see Weeks *et al.*<sup>13</sup>). The 20-site chains have a bond length equal to the site diameter  $l_0 = 1.0\sigma$  and a contour length of  $L = 19\sigma$ . These short-chain polymers have been shown<sup>11</sup> to have a mean-squared end-to-end distance in the melt of  $\langle R^2 \rangle = 29.5(9)\sigma$  and a Kuhn step length of  $b_K = 1.55(5)\sigma$ . These parameters can be related to the dimensions of real polymer molecules using

$$P_b = \frac{LC_\infty}{b_K(\sin(\theta_0/2))^2}, \quad (1)$$

where  $\theta_0$  and  $C_\infty$  are the backbone bond angle and characteristic ratio of the real molecule.  $P_b$  gives the number of backbone carbons in the molecule.

Polypropylene molecules have a bond angle  $\theta_0 = 112^\circ$  (Refs. 14 and 15) and a characteristic ratio  $C_\infty = 5.8$ ,<sup>16</sup> and the propylene monomer, which contains two backbone carbons, has an average molar mass per backbone carbon  $M_m/2 = 21.04$  (where  $M_m$  is the monomeric molar mass). So Eq. (1) shows that the simulated chains can represent (PP) with  $M \approx 2200$  g/mol.

The filler particles are modeled as spheres interacting via a modified WCA potential.<sup>17,18</sup> This interaction includes an expanded core, with diameter  $c_{11}$ , so that their total diameter is  $d = c_{11} + l_0 = c_{11} + 1$ .

All of the distances discussed here are expressed in terms of  $\sigma$ , the position of the Lennard-Jones potential well. Since PP has a bond length  $b_0 = 1.54 \text{ \AA}$ ,<sup>14,15</sup>  $\sigma$  can be calculated, using

$$\sigma = b_0 \sin(\theta_0/2) \left( \frac{P_b}{L} \right), \quad (2)$$

to be  $\sigma = 6.951(6) \times 10^{-10}$  m. This allows the equivalent real diameter of the filler particles to be calculated as  $d = 1.55$  nm when their reduced diameter is  $d = 2.2254\sigma$ .

Masses are reduced using the interaction-site mass  $m$ . The interaction-site mass can be calculated from the parameters given above as

$$m = \frac{P_b M_m}{20 N_A} = 1.807 \times 10^{-22} \text{ g}, \quad (3)$$

where  $M_m = 42.08$  g/mol is the mass of a polypropylene monomer, and  $N_A$  is Avogadro's number.

Energies and temperatures are reduced in terms of the Lennard-Jones potential-well depth  $\epsilon$ , which can be calculated from

$$\epsilon = \frac{\sigma^4}{m(\eta\eta_{\text{real}})^2}, \quad (4)$$

given an estimate of the viscosity of real  $M = 2200$  g/mol PP.

The root-mean-square (rms) radius of gyration of these 20-site chains in the melt has been shown to be  $\langle R_g^2 \rangle^{1/2} = 2.219(2)$  in reduced units.<sup>11</sup> So the ratio of the filler particle radius to the polymer rms radius of gyration, given by  $(d/2)/\langle R_g^2 \rangle^{1/2}$ , is approximately 1/2 for our simulated system.

#### 2. Simulation details

Using a new version<sup>19</sup> of a homogeneous shear nonequilibrium molecular-dynamics<sup>20</sup> program developed by Matin *et al.*, this study simulates a model polymer melt of 20-site polymers interspersed with spherical filler particles in proportions listed in Table I.

The total site number density,  $\rho$ , of each system is adjusted so that each of the various systems experiences approximately the same pressure  $P$ , making the results more

TABLE I. Numbers, ratios, and input properties of the particles simulated: total number of interaction sites  $N$ , number of sites that simulate filler particles  $N_1$ , number of sites that make up polymer molecules  $N_2$ , total number of polymer molecules  $N_p=N_2/20$ , total number of molecules in the system  $N_m=N_1+N_p$ , reduced total pressure  $P$ , reduced interaction-site number density  $\rho$ , and site number fraction of filler  $n_1$ .

$N$	$N_1$	$N_2$	$N_p$	$N_m$	$P(\epsilon/\sigma^3)$	$\rho(m/\sigma^3)$	$n_1$
10 000	0	10 000	500	500	5.251(3)	0.84	0
4664	24	4640	232	256	5.21(12)	0.817	0.005
4303	43	4260	213	256	5.42(15)	0.797	0.010
3695	75	3620	181	256	5.32(15)	0.750	0.020
2897	117	2780	139	256	5.49(16)	0.681	0.040
2384	144	2240	112	256	5.45(15)	0.620	0.060
1757	177	1580	79	256	5.18(16)	0.520	0.101

comparable with experiment. In the choice of a state point, we follow Matin<sup>12</sup> who elected to run his simulations of various-length polymer melts with reduced density  $\rho=0.84(m/\sigma^3)$ , temperature  $T=1.0(\epsilon/k_B)$ , and pressure  $P=5.251(3)(\epsilon/\sigma^3)$  after the work of Johnson and co-workers.<sup>21,22</sup> These authors have shown that this state point produces dense fluid behavior for a range of systems, including short-chain polymers.

These bulk systems are exposed to homogeneous shear rates ranging from  $\dot{\gamma}=0.005(\epsilon/m\sigma^2)^{1/2}$  to  $\dot{\gamma}=0.6(\epsilon/m\sigma^2)^{1/2}$ . From the resulting data, reduced shear viscosities  $\eta$  are calculated using

$$\eta = -\frac{P_{xy}}{\dot{\gamma}}. \quad (5)$$

The components of the pressure tensor are calculated as the average of 100 values which are the output at regular intervals throughout a production run of  $1 \times 10^6$  time steps, with time-step length  $\Delta t=0.002(\epsilon/m\sigma^2)^{-1/2}$ . Uncertainties in  $P_{xy}$  and  $\eta$  are calculated as deviations from these time-averaged values.

The homogeneous shear deformation is applied to the system using the SLLOD algorithm in conjunction with deforming-brick three-dimensional periodic boundary conditions. The details of these algorithms have been described previously<sup>19,20</sup> as have the relevant thermostating issues.<sup>23–26</sup>

## B. Experimental method

For comparison with the simulation data generated in this study, the effect of filler concentration on the steady-state shear behavior of polypropylene filled with 70 nm CaCO<sub>3</sub> spheres was examined experimentally using an advanced rheometrics expansion system (ARES) controlled rate rotational rheometer in the parallel-plate geometry, at a temperature of 210 °C. The samples for steady-shear measurements were prepared as 25 mm disks by compression molding.

The stearic acid treated CaCO<sub>3</sub> nanofiller particles were dispersed in a polypropylene melt, at three different concentrations using a Haake batch mixer. Kao and Bhattacharya<sup>9</sup> gave further details of the method by which the CaCO<sub>3</sub> particles were treated and mixed into the polypropylene. The polymer-filler samples were prepared with concentrations of

15, 25, and 40 wt %, which produce composites with filler volume fractions ( $\phi_1$ ) of approximately 0.054, 0.097, and 0.176.<sup>27</sup>

$$\phi_1 = \frac{(m_1/\rho_1)}{[(m_1/\rho_1) + (1 - m_1)/\rho_2]}, \quad (6)$$

where  $m_1$  is the mass fraction of the filler in the sample, and  $\rho_1 \approx 2800 \text{ kg/m}^3$  and  $\rho_2 \approx 900 \text{ kg/m}^3$  are the approximate densities of the unmixed filler and polymer, respectively.

The polymer used in these experiments has a weight-averaged molar mass of  $M_w \approx 373\,000 \text{ g/mol}$  and a relatively high degree of polydispersity  $M_w/M_n=6.2$  determined by gel permeation chromatography using a Waters Alliance 2000 GPC/V. Since this is much greater than the critical molar mass for entanglement coupling for PP, a textbook estimate of which is  $M_c=7\,000 \text{ g/mol}$ ,<sup>16</sup> these PP samples can be assumed to be in the entanglement regime. This complicates the comparison of experimental to simulation results, since the simulated polymer melt is far from entangled.<sup>11</sup>

Polypropylene molecules in the melt with  $M=373\,000 \text{ g/mol}$  can be assumed (using previously published data<sup>28</sup>) to have a radius of gyration  $\langle R_g^2 \rangle^{1/2}=25.5 \text{ nm}$ . This allows the calculation of the ratio of the filler particle size to the polymer molecule size  $(d/2)/\langle R_g^2 \rangle^{1/2} \approx 2.4$ . This is nearly five times larger than the approximate ratio calculated for the simulated composite. Despite this significant difference of scale, the simulation results are qualitatively compared with the experimental data, as discussed below.

## III. RESULTS

### A. Solution properties of simulated system

The proportion of the filler in each of the simulated systems is calculated as a volume fraction  $\phi_1$  using<sup>17</sup>

$$\phi_1 = \rho n_1 \bar{v}_1, \quad (7)$$

where  $\bar{v}_1$  is the reduced partial volume per particle of the filler. Partial volume is described thermodynamically by

$$\bar{v}_1 = \left( \frac{\partial V}{\partial N_1} \right)_{N_2, T, P}, \quad (8)$$

where  $N_a$  is the number of molecules of component  $a$ . In this study, the partial volume of the filler is estimated as the

TABLE II. Proportion of the filler in the system, stated as an interaction-site fraction  $n_1$  and volume fraction  $\phi_1$ , and the degree of ideality of the solution  $Q$ .

$n_1$	$\phi_1$	$Q$
0.005	0.024	0.878(23)
0.010	0.046	0.863(17)
0.020	0.087	0.724(42)
0.040	0.157	0.511(49)
0.060	0.215	0.285(16)
0.101	0.300	0.196(8)

volume of a sphere with diameter  $d=2.2254\sigma$ , which is  $\bar{v}_1=5.7706$ . Applying this value to Eq. (7) produces the volume fractions listed in Table II. Henceforward, these values of  $\phi_1$  will be used to designate the various polymer-filler systems simulated.

Jolly and Bearman<sup>29</sup> have suggested a means of evaluating an important solution property of a two-component fluid using the structural information available from the radial distribution function of the system. They have shown that a parameter  $Q$  can be used as an indicator of thermodynamic ideality when it is calculated from  $g_{ab}(r)$ ;

$$Q = \left( 1 + \frac{\rho_1 \rho_2}{\rho_1 + \rho_2} (G_{11} + G_{22} - 2G_{12}) \right)^{-1}, \quad (9)$$

where

$$G_{ab} = \int (g_{ab}(r) - 1) d^3r, \quad (10)$$

$r$  is the reduced radius over which the distribution is counted, and  $\rho_a = n_a \rho$  is the site number density of component  $a$ . A value of  $Q=1$  denotes an ideal solution. (In this context, an ideal solution is one where the solution volume is equal to the sum of the component volumes, the relative vapor pressure of each component is proportional to its mole fraction in the solution, the interspecies interaction strengths are equal to the intraspecies interaction strengths, and the components mix evenly with  $\Delta H=0$ .)

Table II lists the results of these fluid-structure-based analyses, and shows that, predictably, the polymer-filler mixture is generally far from ideal at volume fractions greater than 10%, and that ideality is approached as filler content is reduced.

## B. Comparison of viscosities: Simulation and experiment

The zero-shear viscosity of the simulated pure polymer melt has already been shown<sup>11</sup> to be  $\eta_p = (15 \pm 3) \times (\sigma^4/m\epsilon)^{-1/2}$ . The experimental and simulation viscosity results are therefore scaled by these constant  $\eta_p$  values. The zero-shear viscosity of the melt  $\eta_p$  is useful in the evaluation of the relaxation time of the polymer. The modified Rouse theory gives a maximum internal relaxation time for a polymer melt obeying<sup>30</sup>

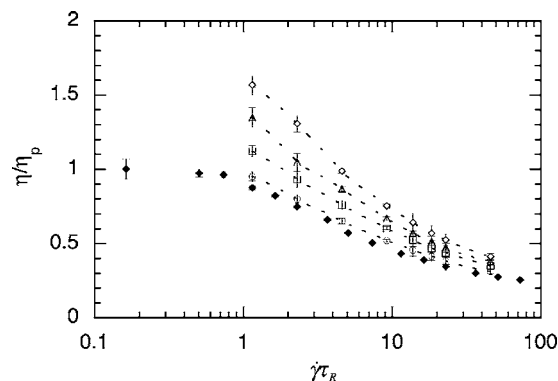


FIG. 1. Shear viscosity  $\eta/\eta_p$  vs shear rate  $\dot{\gamma}\tau_R$ : simulation results, with symbols representing (from top to bottom)  $\phi_1=0.300$  (open diamond),  $\phi_1=0.215$  (open triangle),  $\phi_1=0.157$  (open square),  $\phi_1=0.087$  (open circle), and no filler (solid diamond). The dotted lines interpolate between the data points as a guide for the eye only.

$$\tau_R = \frac{6\eta_p M/N_A}{\pi^2 \rho k_B T}, \quad (11)$$

where  $M/N_A$  is the mass of the molecule ( $N_A$  being Avogadro's number) and  $k_B$  is Boltzmann's constant. Matin<sup>12</sup> used this equation to find a value of  $\tau_R = (230 \pm 10) \times (\epsilon/m\sigma^2)^{-1/2}$  for the simulated 20-site polymers in the melt. These values of  $\eta_p$  and  $\tau_R$  are used to scale the simulation results, to avoid any confusion potentially arising from the use of reduced units.

Figure 1 shows the scaled steady-state shear viscosities as  $\eta/\eta_p$  is plotted against  $\dot{\gamma}\tau_R$ , for the simulated systems under shear. Those systems containing a filler show a strong shear-rate dependence of  $\eta$ , whereas the unfilled polymer exhibits a Newtonian plateau behavior, becoming shear-rate independent, as  $\dot{\gamma}$  is reduced. Over the range of shear rates studied, the shear viscosity consistently increases with filler concentration. The monotonic increase of viscosity with filler concentration is a commonly observed trend in experimental systems. In addition to Kao and Bhattacharya's PP-CaCO<sub>3</sub> studies,<sup>9</sup> this behavior has been observed in a range of polymer-clay systems<sup>1-3,10</sup> and seems to be an important general feature of composites of molten polymers with micron-scale fillers.

The steady-shear results for the real experimental PP-CaCO<sub>3</sub> systems are shown in Fig. 2. Some important differences of scale between the simulated and experimental systems preclude any quantitative comparison between the two sets of results. The ratio  $(d/2)/\langle R_g^2 \rangle^{1/2}$  is five times larger for the real experimental systems than for the simulated ones. The filler particles used in the experiments have around 45 times the diameter of the simulated filler particles. The polymer molecules used in the experiments are estimated to have nearly 170 times the mass of those simulated. These real, macromolecular polymers are likely to be subjected to entanglement effects, which are absent in the simulation of very short chains. Despite these complications, however, some qualitative observations are apposite.

In both the experiment and the simulation the shear viscosities of the filled polymers at each shear rate consistently exceed those of the unfilled polymer, and there is a general



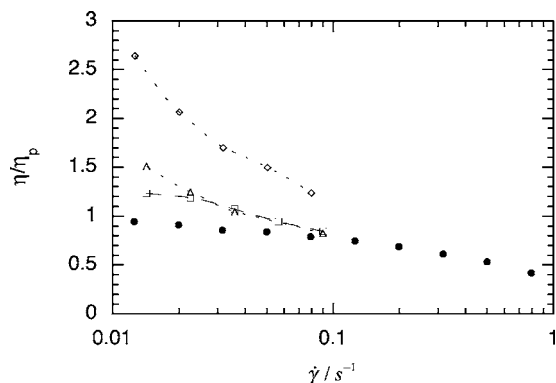


FIG. 2. Shear viscosity  $\eta$  vs shear rate  $\dot{\gamma}$ : experimental results (PP and  $\text{CaCO}_3$  treated with stearic acid), with symbols representing (from top to bottom)  $\phi_1=0.176$  (open diamond),  $\phi_1=0.097$  (open triangle),  $\phi_1=0.054$  (open square), and no filler (solid circle). The dotted lines interpolate between the data points as a guide for the eye only.

trend for viscosity to increase with filler content. Most importantly, Figs. 1 and 2 both clearly illustrate the changes in behavior that occur as filler concentration is varied and suggest a consistent pattern of viscosity gradient growth with filler concentration. For both simulation and experiment, at low filler concentrations the slope in the viscosity curve differs little from that shown by the unfilled polymer, whereas in the systems with the highest filler concentrations, the viscosity varies much more rapidly. These trends are quantified by fitting the power-law regions in the data with the following relationship:

$$\eta = A \dot{\gamma}^B. \quad (12)$$

The values of the parameters  $A$  and  $B$  are listed with their product in Table III and show that the magnitudes of the viscosity exponents ( $|B|$ ) are greater in the more filler-concentrated systems. The gradients of the viscosity curves are related to the product  $AB$  and consistently increase in magnitude with increasing polymer concentration, reflecting the growing rate of shear thinning seen in both the simulated and experimental systems.

An adequate estimate of the zero-shear viscosity of unfilled PP can be made by calculating a weighted linear fit to the viscosity data over the four lowest shear rates. This produces a constant value,  $\eta_p = 10\,714$  Pa s, by which all of the other experimental results can be scaled.

TABLE III. Description of shear viscosity curves: Parameters  $A$  and  $B$  obtained from the power-law fit to the data in Fig. 1 and 2.

System	$\phi_1$	$A$	$B$	$AB$
Simulated polymer-filler	0.0	2.9478	-0.264	-0.7809
Simulated polymer-filler	0.087	3.1513	-0.282	-0.8896
Simulated polymer-filler	0.157	3.4837	-0.295	-1.0270
Simulated polymer-filler	0.215	3.6649	-0.314	-1.1497
Simulated polymer-filler	0.300	3.9541	-0.331	-1.3096
PP- $\text{CaCO}_3$	0.0	5094.7	-0.176	-897.18
PP- $\text{CaCO}_3$	0.054	4920.9	-0.426	-1210.5
PP- $\text{CaCO}_3$	0.097	4167.9	-0.310	-1292.5
PP- $\text{CaCO}_3$	0.176	3657.4	-0.471	-1720.8

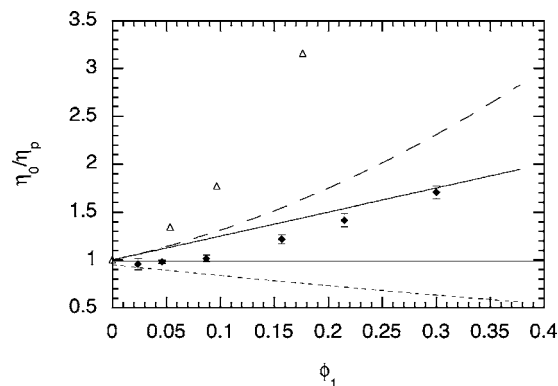


FIG. 3. Zero-shear viscosity  $\eta_0/\eta_p$  vs filler volume fraction  $\phi_1$ . The solid data points represent the simulation results. The open triangles represent the experimental results using PP and  $\text{CaCO}_3$  treated with stearic acid. The horizontal line indicates  $\eta_0 = \eta_p$ . The long-dashed and solid lines indicate the Einstein and Batchelor predictions, respectively. The short-dashed line illustrates the result of Kairn *et al.* (Ref. 11) for the viscosity of a polymer melt with increasing solvent volume fraction.

As expected for systems so different, there is significant quantitative deviation of the simulation results from the experimental data, which is most clearly apparent in the zero-shear viscosity results. Figure 3 shows the zero-shear viscosities of each of the systems calculated by extrapolating the nonequilibrium results to  $\dot{\gamma}=0$ . These results are all scaled by the zero-shear viscosity of the polymer melt  $\eta_p$ , for each system. Note that Fig. 1 does not include the data for the two lowest concentration simulated systems, since they are not sufficiently different from the melt. For reference, Fig. 3 also includes the Einstein,

$$\frac{\eta_0}{\eta_s} = 1 + 2.5\phi_1, \quad (13)$$

and Batchelor,

$$\frac{\eta_0}{\eta_s} = 1 + 2.5\phi_1 + 6.2\phi_1^2, \quad (14)$$

descriptions of the concentration dependence of viscosity in a simple colloidal suspension. Here,  $\eta_p$  is taken to be  $\eta_s$ , the zero-shear viscosity of the solvent.

In a nonpolymeric system, molecular-dynamics simulations have shown that colloidal solute particles with  $d \geq 1.5\sigma$  can increase the viscosity of a solvent of spherical particles.<sup>17</sup> Solvents containing colloidal particles of the size used in the current study ( $d=2.2254\sigma$ ) have been shown to conform with the Einstein relation when  $\phi_1 < 0.048$  and they obey the Batchelor equation when  $\phi_1 < 0.090$ .<sup>17</sup> When the solvent is a polymer, however, these relationships may no longer hold.

Previous research on polymers filled with spherical microparticles (see Shenoy<sup>31</sup>) has shown that, rather than following predictions depending exclusively on  $\phi_1$ , the viscosity of the composite can be sensitive to the size of the filler particles themselves. Smaller-sized spherical filler particles present to the polymer a larger surface area for each  $\phi_1$  than larger particles. High aspect ratio fillers such as clay platelets show increased viscosities at lower concentrations<sup>2,3,10</sup> due to their higher surface area. Similarly, decreasing the size of

spherical filler particles while keeping the filler volume fraction constant is also expected to increase the viscosity of the composite,<sup>31</sup> in some cases resulting in a yield stress. It is reasonable to conclude that this occurs mainly due to the increased polymer adsorption on the filler particles due to the increased available surface area, and is thus associated with strong thermodynamic nonideality of the composite system.

This argument implies that, if the same mechanism were present in the simulated system, the resulting values of  $\eta_0$  might be expected to exceed those identified in the real PP composite at equivalent volume fractions, because the filler particles used in the simulated systems are 45 times smaller than those in the experimental systems. The fact that the opposite is the case, as is evident in Fig. 3, suggests that the mechanism discussed above is absent in our simulated system. It is worth recalling that all the interactions in our simulated systems are short ranged and purely repulsive, so although the filler is well dispersed, attractive interactions between the polymer and filler are absent, unlike the situation for experimental polymer-filler systems. As the simulated filler particles are decreased in size, their effect could be expected to approach that of a plasticizer or solvent, provided that there are no strong attractions between polymer and filler particles.

We have previously examined model polymer solutions using molecular-dynamics simulations. As expected, we found<sup>11</sup> that the polymer solution viscosity decreased with increasing solvent concentration. In this case, the solvent molecules had a diameter equal to the polymer site diameter  $d=1.0\sigma$ . If we relate this to the dimensions of a real filled PP system, as discussed in Sec. II A 1, the model can be shown to represent a filler particle diameter of  $d=6.951(6) \times 10^{-10} \text{ m} \approx 0.7 \text{ nm}$ . Over the entire concentration range, the viscosity of this system was shown to consistently decrease with increasing solvent content, according to

$$\left(\frac{\eta_0}{\eta_p}\right) = \frac{1}{\eta_p}(1.9 + 7.7(1 - \phi_1) + 4.9(1 - \phi_1)^2). \quad (15)$$

This relationship is also illustrated in Fig. 3.

The current study shows that increasing the size of the filler particles by only a small amount, from  $d=1.0\sigma$  to  $d=2.2254\sigma$ , leads to a qualitative change in the effect of the filler on the polymer melt viscosity. The smaller filler particles act to decrease the viscosity while the larger ones increase the viscosity. The change in the viscosity of the filled systems simulated here remains small, but it varies with concentration in the direction expected of “fillers,” rather than “thinners.” Over a threshold concentration of  $\phi_1 \approx 0.3$ , the viscosity of the composite monotonically increases with volume fraction. While the simulation results do not quantitatively relate to the experimental results, these data permit the important qualitative observation, also apparent in Figs. 1 and 2, that the zero-shear viscosity in all of the filled systems increases with their concentration.

#### IV. CONCLUSIONS

This molecular-dynamics simulation study demonstrates that the steady-state shear viscosities of a model polymer

nanocomposite can be usefully compared with experimental results for real polymer composites. The difference in scale between the simulated systems and the composites examined experimentally precludes quantitative comparisons of the results, but several qualitative similarities in shear rheology are evident. Both the simulated and the experimental systems examined here show that where the shear viscosities of the filled systems differ from those of the pure polymer they consistently exceed them, with increased viscosities resulting from increasing the filler content in the composite. They also both exhibit a trend towards stronger shear-thinning behavior as the proportions of the filler are increased.

This steeper shear thinning observed in the viscosities of the more filled systems is comparable with the results of experiments on polymer composites containing a nonspherical filler. Various studies of polymers filled by platelet particles have concluded that the dispersion of filler particles through the polymer matrix leads to interactions which increase the viscosity of the composite, and that increasing the filler content amplifies this effect.<sup>2,3,32</sup> The results of our simulations of composites with spherical filler particles also conform with this conclusion. However, we do not observe the strong increase in viscosity with decreasing filler size at constant filler volume fraction that is sometimes observed experimentally. This difference probably occurs because the particles in our model experience purely repulsive interactions, in contrast with the experimental systems which exhibit strong attractive interactions between the polymer and filler. This conclusion is strengthened by a comparison with the molecular-dynamics simulations of polymer-nanoparticle systems by Starr *et al.*<sup>8</sup> which showed that greater dispersion of the nanoparticles produced a larger viscosity for the same filler volume fraction when strong attractive interactions were present.

One of the most interesting results of our simulations is the conclusion that a small change in the particle size of filler particles can qualitatively change the concentration dependence of the viscosity. When particles the same size as the polymer beads are added to the polymer melt, the particles act as a solvent or a plasticizer and the viscosity decreases, but if the added particles are only slightly bigger than twice the size of the polymer beads, the viscosity increases with increasing filler concentration. In the current simulations, the ratio of the particle radius to the polymer rms radius of gyration is approximately 1/2. A reduction in the viscosity of a polymer nanocomposite has been observed in the experimental system studied by Mackay *et al.*,<sup>33</sup> in which crosslinked polymer nanoparticles and a polymer melt were blended. The particle size to polymer size ratio in the experimental system was estimated as being of the order of 0.5 up to 1.0 (i.e., similar to ours), and the nanoparticles were described as “soft spheres.” Enthalpic effects were deliberately minimized by dispersing crosslinked polystyrene nanoparticles in a polystyrene melt. Our results for the two particle sizes considered (“polymer nanoparticle” and “polymer solvent”) confirm the trends shown by the experimental results and qualitatively agree with the suggestion by Mackay *et al.* that free-volume (i.e., packing) effects are largely responsible for the decrease of the viscosity when very small nanoparticles are

added to a polymer melt. Our observation that the concentration dependence of the viscosity can change from being free-volume dominated (solventlike) to hydrodynamics dominated (fillerlike) within such a small range of nanoparticle sizes warrants further investigation.

Concluding, it seems that simulations can replicate the main features of the viscometric behavior of filled-polymer systems, even when the dimensions involved are on a completely different scale. We have already commenced an extension of this work in which we simulate composites with polymer chains ten times the length of those examined here, and we intend to compare the resulting data with the results of rheological experiments on composites containing filler particles of submicron size. A more direct comparison of experiment and simulation of filled-polymer systems is now foreseeable.

## ACKNOWLEDGMENTS

This work was supported by RMIT's Virtual Research and Innovation Institute for Information and Communication Technology, through a grant from the Research Investment Fund, and by a grant from the Victorian Partnership for Advanced Computing through the e-Research Scheme. The Australian and Victorian Partnerships for Advanced Computing also assisted with generous allocations of computer time. Two of the authors (T.K.) and (P.J.D.) would especially like to thank the other members of the Rheology and Materials Processing Centre's nanocomposites group for a valuable introduction to the practicalities of polymer composite rheology, as well as for their ongoing support and advice.

<sup>1</sup>R. Krishnamoorti, R. A. Vaia, and E. P. Giannelis, *Chem. Mater.* **8**, 1728 (1996).

<sup>2</sup>H. J. Choi, G. K. Seong, Y. H. Hyun, and M. S. Jhon, *Macromol. Rapid Commun.* **22**, 320 (2001).

<sup>3</sup>R. Prasad, V. Pasonovic-Zujo, R. K. Gupta, F. Cser, and S. N. Bhattacharya, *Polym. Eng. Sci.* **44**, 1220 (2004).

<sup>4</sup>R. K. Bharadwaj, R. A. Vaia, and B. L. Farmer, in *Nanocomposites: Synthesis, Characterisation, and Modeling*, edited by R. Krishnamoorti and R. A. Vaia (American Chemical Society, Washington, D.C., 2002).

<sup>5</sup>J. S. Smith, D. Bedrov, and G. D. Smith, *Compos. Sci. Technol.* **63**, 1599 (2003).

<sup>6</sup>S. J. V. Frankland, V. M. Harik, G. M. Odegard, D. W. Brenner, and T. S. Gates, *Compos. Sci. Technol.* **63**, 1655 (2003).

<sup>7</sup>J. Y. Lee, A. R. C. Baljon, R. F. Loring, and A. Z. Panagiotopoulos, *J. Chem. Phys.* **109**, 10321 (1998).

<sup>8</sup>F. W. Starr, J. F. Douglas, and S. C. Glotzer, *J. Chem. Phys.* **119**, 1777 (2003).

<sup>9</sup>N. Kao and S. Bhattacharya, Proceedings of the Eight National Conference on Rheology, Adelaide, Australia, 19–22 July 1998 (unpublished).

<sup>10</sup>M. J. Solomon, A. S. Almusallam, K. F. Seefeldt, A. Somwangthanaroj, and P. Varadan, *Macromolecules* **34**, 1864 (2001).

<sup>11</sup>T. Kairn, P. J. Daivis, M. L. Matin, and I. K. Snook, *Polymer* **45**, 2453 (2004).

<sup>12</sup>M. L. Matin, Ph.D. thesis, RMIT University, 2001.

<sup>13</sup>J. D. Weeks, D. Chandler, and H. C. Andersen, *J. Chem. Phys.* **54**, 5237 (1971).

<sup>14</sup>T. Asakura, I. Ando, and A. Nishioka, *Makromol. Chem.* **177**, 1493 (1976).

<sup>15</sup>U. W. Suter and P. J. Flory, *Macromolecules* **8**, 765 (1975).

<sup>16</sup>J. Karger-Kocsis, *Structure and Morphology*, Polypropylene: Structure, Blends and Composites Vol. 1 (Chapman and Hall, London, 1995).

<sup>17</sup>M. McPhie, Ph.D. thesis, RMIT University, 2003.

<sup>18</sup>I. Snook, B. O'Malley, M. McPhie, and P. Daivis, *J. Mol. Liq.* **103–104**, 405 (2003).

<sup>19</sup>M. L. Matin, P. J. Daivis, and B. D. Todd, *Comput. Phys. Commun.* **151**, 35 (2003).

<sup>20</sup>D. J. Evans and G. P. Morriss, *Statistical Mechanics of Nonequilibrium Liquids* (Academic, London, 1990).

<sup>21</sup>J. K. Johnson, J. A. Zollweg, and K. E. Gubbins, *Mol. Phys.* **78**, 59 (1993).

<sup>22</sup>J. K. Johnson, E. A. Mueller, and K. E. Gubbins, *J. Phys. Chem.* **98**, 6413 (1994).

<sup>23</sup>S. Bair, C. McCabe, and P. T. Cummings, *Phys. Rev. Lett.* **88**, 058302 (2002).

<sup>24</sup>K. P. Travis, P. J. Daivis, and D. J. Evans, *J. Chem. Phys.* **103**, 10638 (1995).

<sup>25</sup>K. P. Travis, P. J. Daivis, and D. J. Evans, *J. Chem. Phys.* **103**, 1109 (1995).

<sup>26</sup>P. Padilla and S. Toxvaerd, *J. Chem. Phys.* **104**, 5956 (1996).

<sup>27</sup>N. Kao, A. Chandra, and S. Bhattacharya, *Polym. Int.* **51**, 1385 (2002).

<sup>28</sup>J. Brandrup, E. H. Immergut, and E. A. Grulke, *Polymer Handbook* (Wiley, New York, 1999).

<sup>29</sup>D. L. Jolly and R. J. Bearman, *Mol. Phys.* **41**, 137 (1980).

<sup>30</sup>J. D. Ferry, *Viscoelastic Properties of Polymers* (Wiley, New York, 1980).

<sup>31</sup>A. V. Shenoy, *Rheology of Filled Polymer Systems* (Kluwer, Dordrecht, 1999).

<sup>32</sup>Y. T. Lim and O. O. Park, *Rheol. Acta* **40**, 220 (2001).

<sup>33</sup>M. E. Mackay, T. T. Dao, A. Tuteja, D. L. Ho, B. van Horn, H.-C. Kim, and C. J. Hawker, *Nat. Mater.* **2**, 762 (2003).